Delft University of Technology

Infragravity waves and bore merging

Tissier, Marion; Bonneton, P; Ruessink, Gerben

INFRAGRAVITY WAVES AND BORE MERGING

Marion Tissier[1], Philippe Bonneton[2] and Gerben Ruessink[3]

Abstract

The phenomenon of bore merging is investigated using two high-resolution laboratory experiments including bichromatic and irregular wave conditions. The locations at which waves start merging are identified and the hydrodynamic conditions in the vicinity of the merging points are examined. Bore merging takes place in the inner surf zone for all conditions considered. The infragravity- to short-wave height ratio is close to or larger than one at the merging point, indicating that bore merging occurs in a part of the surf zone that is already dominated by the infragravity waves. Our data analysis is supplemented by numerical simulations that confirms the importance of infragravity waves in the occurrence bore merging. Moreover, our simulations suggest that bore merging has a very limited effect on the infragravity wave field. This casts doubts on the importance of bore merging as an infragravity wave generation mechanism.

Keywords: bore merging, infragravity wave generation, short and long wave interaction, surf zone dynamics

1. Introduction

Bore merging (i.e. faster bores overtaking slower ones and merging) is commonly observed in natural surf zones, and can modify significantly the wave field. Sénéchal *et al.* (2001a,b) have for instance shown that it could lead to a significant increase of the wave period in the cross-shore direction, with the observation of periods larger than twice the offshore mean period in the inner surf zone. This lead them to hypothesize that bore merging could be a source of infragravity wave energy, although they recognized that this effect was weak for their dataset. Bore merging was subsequently mentioned as a source of infragravity wave energy in several studies (e.g., Brocchini and Baldock, 2008), but the importance of this generation mechanism has never been quantified.

On the whole, very few studies have analyzed bore merging. As a result, the mechanisms leading to bore merging are still not well understood. Bore merging is commonly associated to the phenomenon of amplitude dispersion, i.e. the fact that larger waves propagate faster and can therefore overtake smaller bores (e.g., Sénéchal et al. 2001, Brocchini and Baldock, 2008). Early field observations suggest that bore merging occurs predominantly in the surf zone of low sloping beaches (e.g., Huntley and Bowen, 1975), where the variability in wave height is expected to decrease significantly due to the propagation over a wide surf zone. On these mildly sloping beaches, infragravity waves can be very energetic in shallow water (e.g. Ruessink *et al.*, 1998) and influence short-wave dynamics (Abdelrahman and Thornton, 1987; van Dongeren *et al.*, 2007).

In a recent study we have shown that, for a set of bichromatic wave experiments, the intra-wave variability in short-wave celerity was mainly controlled by the variations in water level and velocity induced by the infragravity waves (Tissier *et al.*, 2015). Short-waves propagating on the incoming infragravity wave crest were seen to travel consistently faster than the waves propagating on the troughs due to the increased water level and the positive current associated with the orbital velocity of the infragravity wave. This suggests that the infragravity waves themselves could be responsible for bore convergence in the surf zone, and therefore merging. This study, however, did not entirely rule out the role

[1] Dept. Hydraulic Engineering, Faculty of Civil Engineering and Geosciences, Delft University of Technology, Delft, The Netherlands, m.f.s.tissier@tudelft.nl
[2] UMR EPOC, University of Bordeaux, Talence 33405, France, p.bonneton@epoc.u-bordeaux1.fr
[3] Dept. Physical Geography, Faculty of Geosciences, Utrecht University, The Netherlands, g.ruessink@uu.nl

of amplitude dispersion, as infragravity wave modulation of the water level in the surf zone was associated to a modulation of the short-wave height, with larger waves predominantly located on the infragravity wave crests.

In the present paper, we investigate further the relation between bore merging and infragravity waves. The laboratory data used in Tissier *et al.* (2015) will be extended to include irregular cases and used to characterize the conditions in which bore merging occurs. Finally, our data analysis will be supplemented by some numerical modelling to further investigate the role played by the infragravity waves in the occurrence of merging. The relevance of bore merging as an energy transfer mechanism will also be discussed based on our numerical results.

2. Methods

2.1. Laboratory experiments

This study analyzes data collected during two small-scale laboratory experiments designed to investigate short and infragravity wave transformation over mildly sloping beaches. The final dataset analyzed in the present study consists of 11 bichromatic wave conditions and 7 irregular wave conditions, over planar beaches of slope 1/35 (van Noorloos (2003) experiment) and 1/80 (GLOBEX experiment, Ruessink *et al.,* 2013 and Michallet *et al.,* 2014). An overview of the wave conditions considered in this study is provided in Table 1. For both experiments, high-resolution (in space and time) synchronized measurements of surface elevation are available (see measurement locations in Figure 1), allowing us to track and characterize individual waves during their propagation towards the shore (see Section 2.2.2).

Table 1. Offshore wave conditions for the 18 cases considered. a_1 and a_2 (f_1 and f_2) are the amplitudes (frequencies) of the primary wave components for the bichromatic wave cases. The irregular wave cases are characterised here by their significant wave height (H_s) and peak period (T_p).

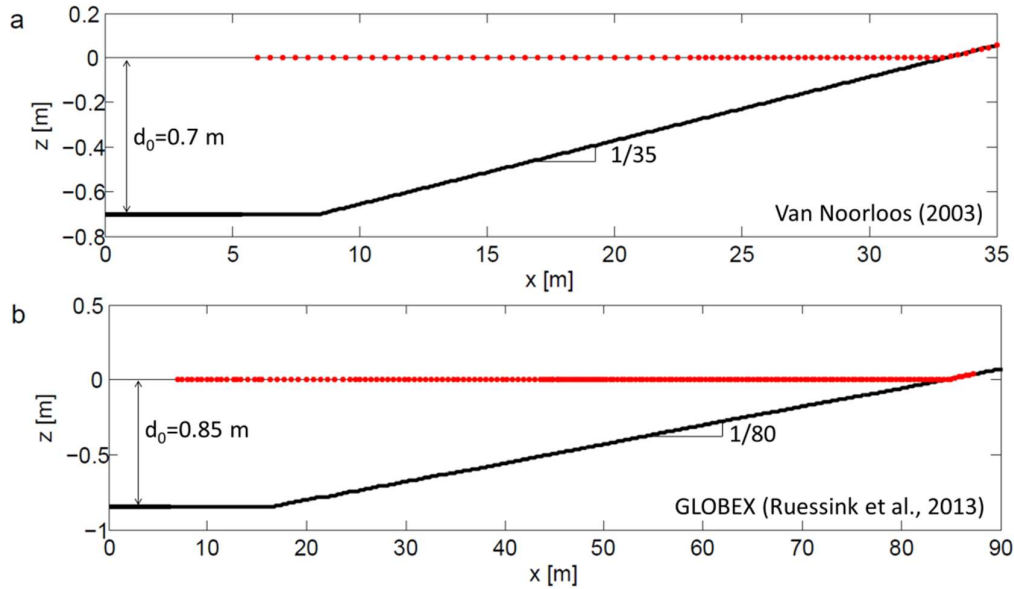| Bichromatic waves	Case name	a_1 (m)	a_2 (m)	f_1 (Hz)	f_2 (Hz)
GLOBEX	G1	0.09	0.01	6/15	7/15
- 1/80 slope	G2	0.09	0.01	0.42	0.462
	G3	0.07	0.03	0.42	0.462
Van Noorloos	A1			0.6714	0.4761
- 1/35 slope	A2			0.6470	0.5005
	A3	0.06	0.012	0.6348	0.5127
	A4			0.6226	0.5249
	B1	0.06	0.018		
	B2	0.06	0.024		
	B3	0.06	0.030	0.6470	0.5005
	B4	0.06	0.036		
Irregular waves	Case name	H_s (m)	T_p (s)	-	-
GLOBEX	I1	0.10	1.58		
- 1/80 slope	I2	0.20	2.25		
	I3	0.10	2.25		
Van Noorloos	C1	0.05	2.00		
- 1/35 slope	C2	0.075	2.00		
	C3	0.10	2.00		
	D1	0.05	1.54		

Figure 1. Experimental set-up for the two datasets considered in this study. Bed profile (thick black line) as a function of the cross-shore coordinate x (x=0 at the wave maker) for the van Noorloos' experiment (a) and the GLOBEX experiment (b). The locations where the surface elevation was measured are indicated by the red dots.

2.2. Data analysis

2.2.1. Localization of bore merging

Space-time diagrams of free-surface elevation are first built for each wave condition. Figure 2 shows two examples of such diagrams, for the bichromatic case A1 (Fig. 2a) and the irregular wave case I3 (Fig. 2b). The locations where waves start to merge are identified directly from these diagrams as the points where the crest trajectories (light gray lines in Fig. 2a,b) converge and merge (circles in Fig. 2a,b). A given wave can merge consecutively with several waves in the surf zone. In the following, we focus on the locations where the first merging occurs, indicated by red circles in Figures 2a and 2b. This cross-shore location can vary in time for a given experiment from one wave group to the next, especially for the irregular wave cases (e.g., Fig. 2b). For each wave condition, we define the mean location at which merging starts, $x_{merging}$ as the average of the individual merging points over the entire time-series for the irregular wave cases, and over 1-3 wave groups for the bichromatic cases.

2.2.2. Individual wave characteristics

Individual wave characteristics are calculated for each experiment following the method introduced in Tissier *et al*. (2015). The main steps are summarized below. Individual wave crests are identified offshore and tracked during their propagation towards the shore. For each tracked wave and at each cross-shore position, the wave trough is identified as the first local minimum of surface elevation preceding the crest. The individual wave height H_i is then defined as the difference in elevation between the crest and the trough, and the individual wave period as the duration separating two consecutive crests. This simple crest tracking procedure is efficient for bichromatic wave conditions (Tissier *et al*., 2015), but less suited for strongly irregular wave cases. To limit the tracking errors, we focus the analysis on waves with H_i larger than 2 cm at our most offshore point, and exclude waves that, according to our analysis, reach values less than 5 mm offshore of the mean breakpoint.
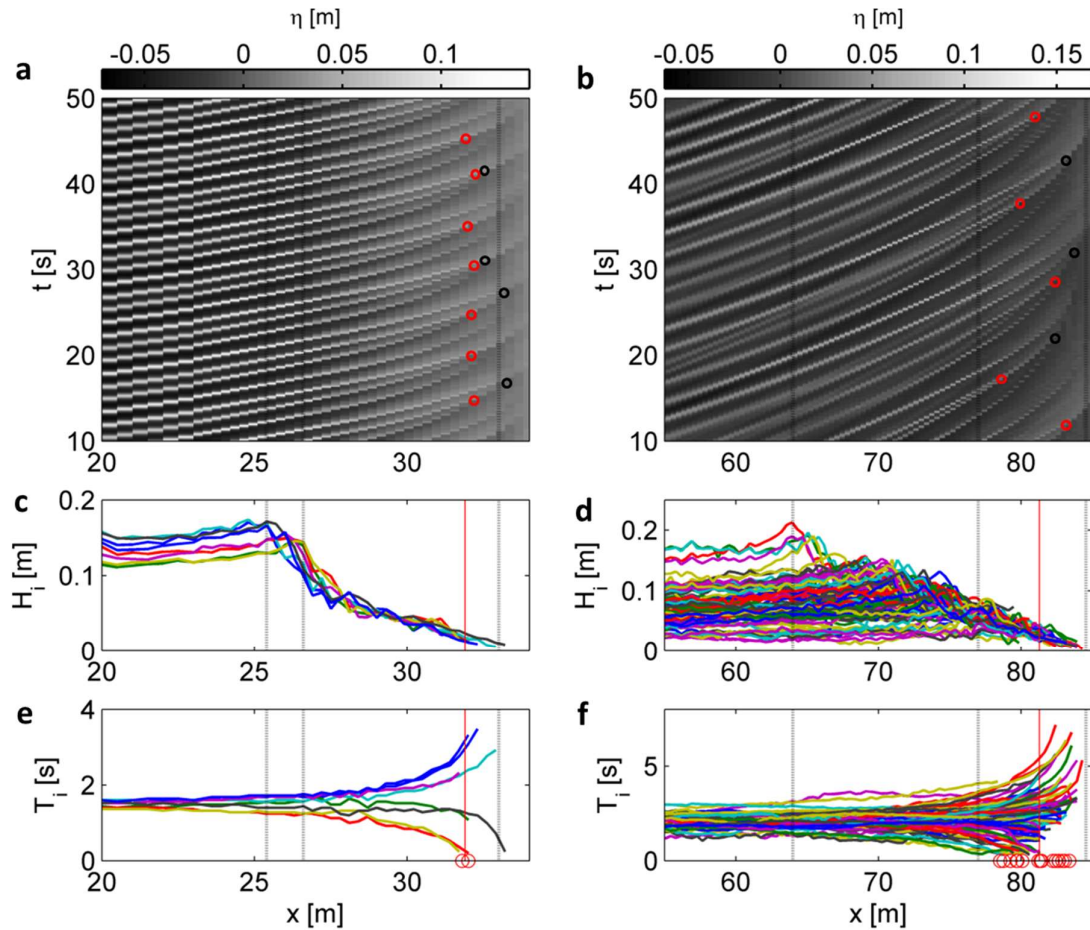
Figure 2. (a-b) Space-time diagrams of the free-surface elevation (η) and (c-f) individual wave characteristics as a function of the cross-shore distance x for bichromatic wave case A1 (left panel, 9 waves followed, i.e. 3 wave groups) and for irregular wave case I3 (right panel, 94 waves identified). The red circles in panels a-b indicate the location where waves merge for the first time, while the black circles show examples of secondary merging points (not analyzed in the present study). Each colored line in panels c-f represents one individual wave. The vertical dashed lines indicate, from left to right, the first breakpoint location, the last breakpoint location and the position of the still waterline. The red circles in panels e-c indicate the locations where the waves start merging. The vertical red line is the mean merging position x_{merging}.

3. Results

3.1. Bore convergence and occurrence of merging

The cross-shore evolution of H_i and T_i is shown in Figure 2 (c-f) for cases A1 (left) and I3 (right). As expected, the variability in wave height is much larger for the irregular wave case (Fig. 2d) than for the bichromatic case (Fig. 2c), and decreases significantly once all the waves are broken ($x>27$ m for A1, $x>17$ m for I3, indicated by the second vertical dotted line). It can be noticed that some variability in H_i remains in the inner surf zone. There, the modulation in short-wave height is positively correlated with the (incoming) infragravity wave elevation, with larger waves preferentially located at the infragravity crests (see correlation coefficient between short-wave envelop and infragravity wave elevation in Fig. 3c-d). The

importance of amplitude dispersion for the occurrence of bore merging will be discussed in Section 4.

The cross-shore change in individual wave periods (Fig. 2e,f) is particularly interesting, as it allows us to visualize the convergence/divergence of the wave crests, that ultimately leads to bore merging. The overall evolution of T_i is similar for all wave cases (bichromatic and irregular) considered in this study. The individual wave periods stay relatively constant in the shoaling zone, but start diverging when the waves enter the surf zone, at a rate that increases when the water becomes shallower. The period of a given wave decreases when it is catching up with the previous one, and tends to zero when two consecutive waves merge. This happens around $x \approx 32\ m$ in case A1 for instance (Fig. 2e), which corresponds also to the merging locations calculated from the space-time diagrams (red circles in Fig. 2e and 2f). For the irregular wave case I3, the cross-shore coordinate of the merging points varies significantly in time. It can be noted that the merging points are not always associated with a decrease in T_i (Fig. 2f). This indicates that our crest tracking algorithm failed (and therefore stopped) before the waves reached the merging point. This happens when two wave crests get too close to each other and thus cannot be differentiated anymore, or when the followed crest becomes too low.

Bore merging occurs in the surf zone for 17 wave conditions out of 18 (all wave cases except G2). To compare the different cases, we introduce a normalized depth d^* such as $d^*=d/d_{breaking}$, where $d_{breaking}$ is the still water depth at the mean breakpoint location (defined such as $d^*<1$ in the surf zone and $d^*=0$ at the still water line). The normalized water depth at the mean merging location, $d^*_{merging}$, varies between 0 and 0.36 for the cases considered in this study, which means that bore merging always starts in the inner half of the surf zone ($d^*<0.5$).

3.2. Energy distribution at the merging point

In the following we examine the energy distribution between the short- and infragravity-wave frequency bands in the vicinity of $x_{merging}$. The short ($H_{s,hf}$) and infragravity ($H_{s,lf}$) significant wave heights are calculated using half the offshore peak frequency as cut-off frequency ($f_{cut} = f_1/2$ for the bichromatic wave experiments). Figures 3a and 3b show the cross-shore evolution of these wave heights for cases A1 and I3. On the whole, no significant change in these bulk parameters can be observed in the vicinity of the mean merging point, even in the bichromatic cases where bore merging happens at a (quasi) fixed location (e.g., Fig. 3a). Interestingly, the mean merging point (red vertical line) is systematically located in a part of surf zone where infragravity waves are as energetic as the short waves ($H_{s,lf}\approx H_{s,hf}$) or are already dominating the hydrodynamics ($H_{s,lf}>H_{s,hf}$). Averaged over the 17 cases, $H_{s,lf}/H_{s,hf}=1.4$ at $x=x_{merging}$, with a standard deviation of 0.43.

The relation between relative infragravity wave height and bore merging is further illustrated in Figure 4. This figure shows that the normalized depth at which bore merging starts, $d^*_{merging}$, and the normalized depth at which $H_{s,lf}/H_{s,hf}=1$ are positively correlated, with a coefficient $R^2=0.68$. The ratio of infragravity wave height to short wave height seems therefore to be a good proxy for estimating the mean merging location. This also suggests that the occurrence of merging, easily quantified using remote-sensing techniques for instance, could be an indirect way to get information about the infragravity wave field. More specifically, it could give a first estimate of the value of $H_{s,lf}/H_{s,hf}$, which was shown to be a good indicator for infragravity sand transport mechanisms and direction for instance (de Bakker *et al.,* 2016).
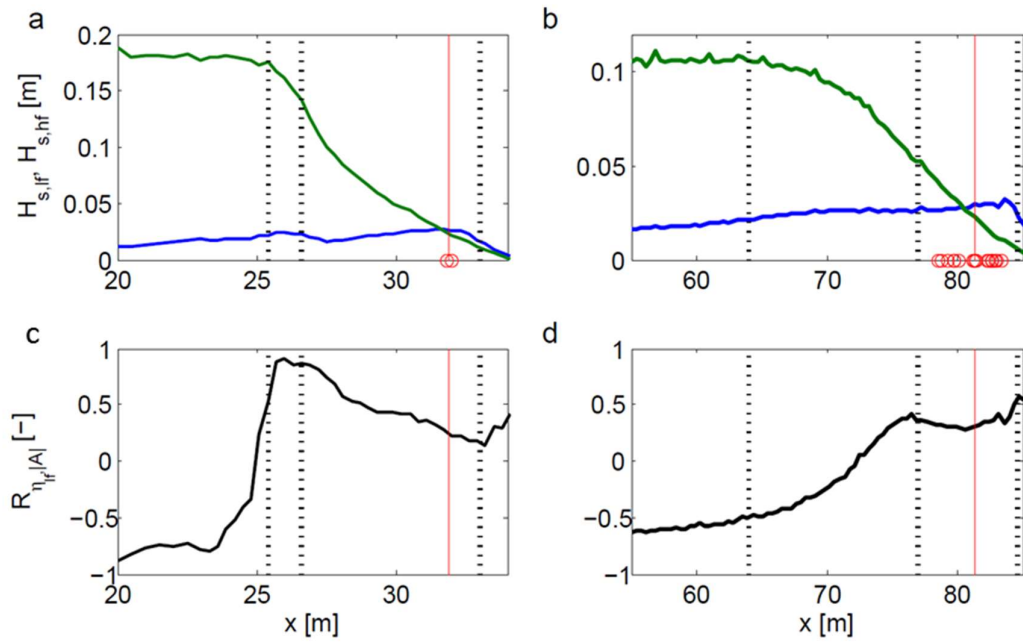
Figure 3. Conditions at the merging point for the bichromatic case A1 (left column) and the irregular wave case I3 (right column). (a, b) Cross-shore evolution of the short (green line) and infragravity (blue line) significant wave heights. (c, d) Correlation coefficient $R_{\eta_{lf},|A|}$ between the infragravity wave elevation η_{lf} and the short-wave envelope $|A(t)|$, calculated following Janssen *et al.* (2003). The average location at which the first waves start merging is indicated by the red vertical lines.
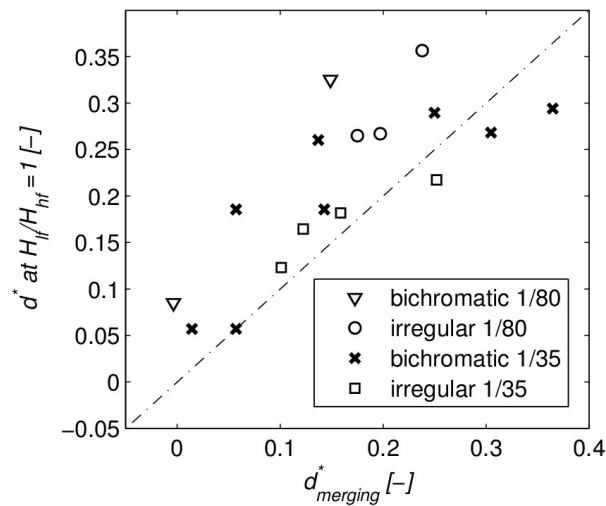

Figure 4. Normalized depth $d^*=d/d_{breaking}$ at which the ratio of the infragravity to the short wave heights is equal to 1 as a function of the normalized depth at the initiation of merging for all wave conditions except G2. The dashed line indicates the 1:1 relationship.

456

4.   Discussion

4.1. Mechanisms leading to bore merging

Tissier *et al.* (2015) have shown that the low-frequency modulation of water depth and velocity induced by the infragravity waves explained most of the intra-wave variability in celerity. This lead them to hypothesize that amplitude dispersion played a secondary role. The data analysis performed in the present study confirms that infragravity waves generated outside the inner surf zone play an important role on bore merging processes, even in more realistic irregular wave cases. However, it does not allow us to rule out the role of amplitude dispersion, as the presence of infragravity waves also results in a modulation of the short-wave height. For all cases considered, the correlation between short-wave envelop and infragravity wave elevation is indeed positive at the location where bore merging starts (see examples in Fig. 3c,d). This wave height modulation is expected to enhance the differences in celerity between the waves located at the infragravity wave crest and trough, and therefore contribute to merging.

To gain more insight into the relative importance of these mechanisms, we perform a series of numerical simulations using a nonlinear shallow water model (Marche *et al.*, 2008). The shock-capturing properties of this model allows for accurate predictions of wave breaking dissipation and shoreline motion without any ad-hoc parametrization, making it an ideal tool to simulate wave transformation in the surf and swash zones.

As we have seen in Sections 3.1 and 3.2 that bichromatic and irregular wave cases behave similarly in terms of bore convergence, we focus here on bichromatic wave conditions for the sake of simplicity. The reference simulation corresponds to the bichromatic case A1. The bed profile is the same as the experimental one (Fig. 1a) but starts at x=29.9 m. The offshore boundary of our model is therefore located well-inside the experimental surf zone (see measured wave heights in Fig. 2c), but offshore of the first merging point (Fig. 2e). For this reference simulation, we impose the measured surface elevation at the offshore boundary of our numerical model. The left panel of Figure 5 compares the predicted surface elevation time-series to the measurements at different cross-shore locations. The model outputs (blue lines) are in close agreement with the data (red lines). It predicts the fast convergence and merging of the wave fronts leading to a significant decrease of the number of waves at the shallowest locations (see dashed lines).

We then perform a second simulation in which we filter out the infragravity wave component at the offshore boundary condition. Because we are focusing here on very shallow water depths, where even the infragravity waves behave strongly non-linearly, there is no clear frequency separation between short- and infragravity waves anymore. The infragravity wave component is therefore defined following van Dongeren *et al.* (2007) as the component of frequency f_1-f_2 and its higher harmonics (thick blue line in Fig. 5a, left panel). The results of this second simulation are shown in the right panel of Figure 5. In that case, the rate at which the waves are converging decreases strongly, confirming that bore merging is strongly influenced by the infragravity wave field generated outside of surf zone. This demonstrates that amplitude dispersion plays only a secondary role in this case, as the intra-wave variability in celerity due to the variability in individual wave height is insufficient to lead to bore merging.

4.2. Source of infragravity wave energy?

We have demonstrated that infragravity waves generated seaward of the inner surf zone play a leading role in the initiation of bore merging. Here we discuss the consequence of this merging on the infragravity waves themselves. We perform a third numerical simulation similar to the previous ones in terms of bathymetry and offshore water level, but now only generate infragravity waves at the offshore boundary.

The surface elevation time-series imposed at the offshore boundary of our model is obtained as in Section 4.1, i.e. we filter the surface elevation measured at x=29.9 m for case A1 to keep only the component of frequency f_1-f_2 and its multiples. The model outputs are compared in Figure 6 with the infragravity waves predicted by the model in the reference simulation (i.e. the simulation including both short and infragravity waves). On the whole, the transformation of the infragravity waves are very similar, irrespective of the presence or absence of the short waves. The infragravity waves progressively steepen when they propagate through the (short-wave) inner surf zone until they break and decrease in height. The

most significant differences between the time-series can be found at the shallowest locations (see Fig. 6g-h). The steepening of the long-wave is for instance slightly more pronounced for the simulation excluding short-waves. This difference can be explained by the absence of short-wave induced set-up, which results in a lower water depth close to the shoreline.

On the whole, our results show that most of the infragravity wave energy found close to the shoreline can be explained by the non-linear transformation of the infragravity waves generated seaward of the inner surf zone. Although additional analyses will be required to generalize our findings, this suggests that the convergence and merging of the short waves has a very limited effect on infragravity wave dynamics in the inner surf zone.
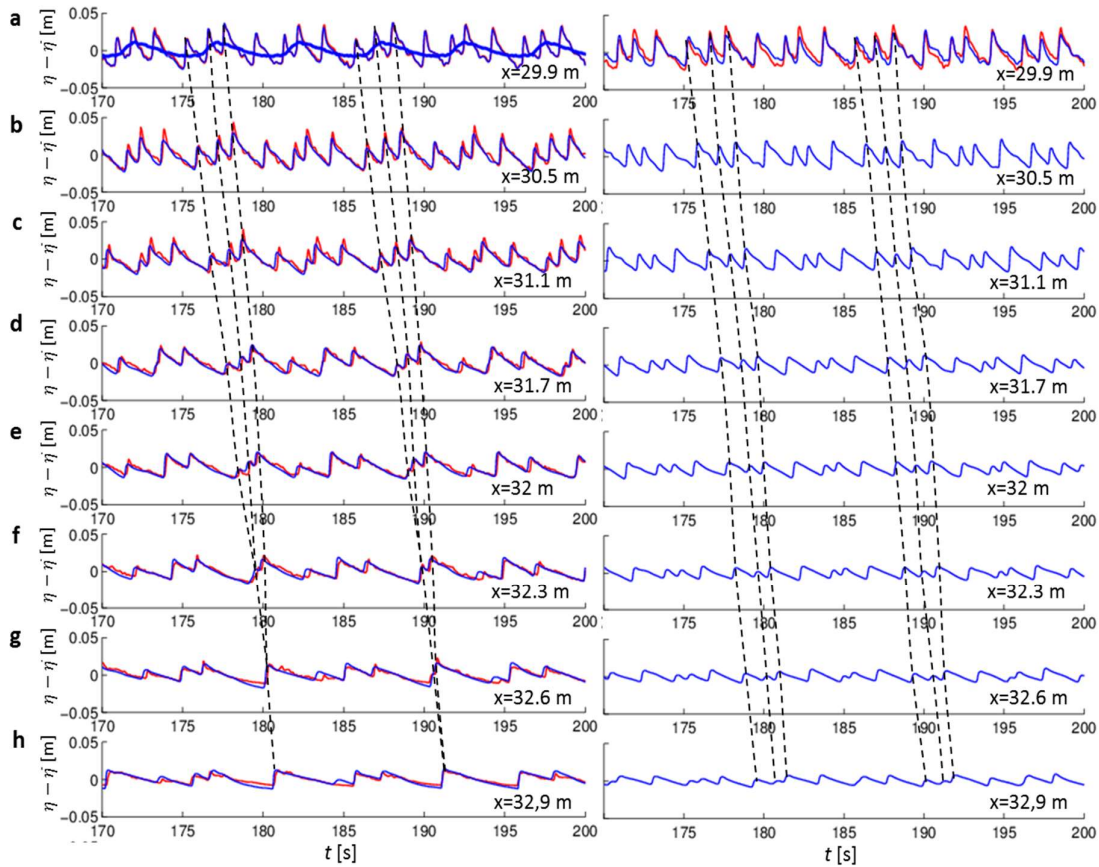

Figure 5. Modelled (thin blue lines) and measured (red lines) surface elevation time-series at different locations within the surf zone, from x=29.9 m (a) to x=32.9 m (h) for case A1, with (left) and without (right) infragravity waves at the offshore boundary condition (x=29.9 m, panel (a)). The thick blue line in (a) shows the infragravity wave signal (defined as the component of frequency f_1-f_2 and its multiples) that is filtered out at the boundary for the second simulation (left panel). The elevation time-series are defined with respect to the mean water level $\bar{\eta}$.
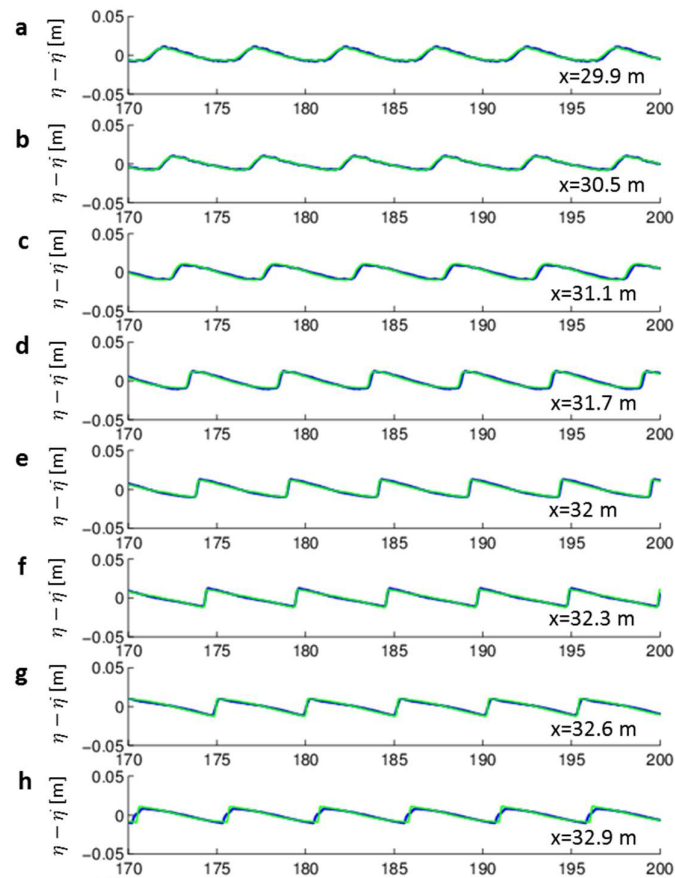
Figure 6. Infragravity wave time-series at different locations within the inner surf zone obtained from a simulation with (blue lines, reference simulation) and without (green lines) short waves at the offshore boundary (x=29.9 m). The blue lines are the infragravity wave component of the total surface elevation shown in Fig. 5, defined as the component of frequency f_1-f_2 and its multiples. The surface elevation time-series are defined with respect to the mean water level $\bar{\eta}$.

5. Conclusions

High-resolution surface elevation measurements collected during two laboratory experiments were analysed to gain insight into the mechanisms leading to bore merging and the role of infragravity waves in this process. Our final dataset includes a large range of incoming wave conditions, including bichromatic and irregular wave cases. For all cases, individual waves start converging when they enter the surf zone, at a rate that increases with decreasing water depth. This convergence leads to bore merging in the inner surf zone in 17 out of 18 cases considered.

No significant changes in the time-averaged energy distribution between the short- and infragravity frequency bands could be identified at the location where the merging process starts. Interestingly, the infragravity- to short-wave height ratio was close to one at the first merging point for all wave conditions considered. This indicates that bore merging occurs in a part of the surf zone where infragravity waves are already dominating. On the whole, our results confirm that infragravity waves are responsible for the occurrence of bore merging, but do not provide any evidence supporting the role of bore merging in the generation of infragravity wave energy.

Acknowledgements

References

Abdelrahman, S.M. and E.B. Thornton, 1987. Changes in the short-wave amplitude and wave-nuber due to infragravity waves, *Coastal Hydrodynamics Conference*, edited by R.A. Dalrymple, ASCE

de Bakker, A. T. M., J. A. Brinkkemper, F. van der Steen, M. F. S. Tissier, and B. G. Ruessink, 2016. Cross-shore sand transport by infragravity waves as a function of beach steepness, *Journal of Geophysical Research: Earth Surface,* 121, 1786–1799, doi:10.1002/2016JF003878.

Brocchini, M. and T. E. Baldock, 2008. Recent advances in modeling swash zone dynamics: Influence of surf-swash interaction on nearshore hydrodynamics and morphodynamics, *Review of Geophysics, 46, RG3003, doi:10.1029/2006RG000215.*

Van Dongeren, A., Battjes, J., Janssen, T., Van Noorloos, J., Steenhauer, K., Steenbergen, G., and Reniers, A. J. H. M., 2007. Shoaling and shoreline dissipation of low-frequency waves. *Journal of Geophysical Research: Oceans*, *112*(C2).

Huntley D. A. and Bowen A. J., 1975. Comparison of the hydrodynamics of steep and shallow beaches. In: J.R. Hails and A. Carr (eds.) *Nearshore Sediment Dynamics and Sedimentation*. Wiley, London, 69-109.

Janssen, T. T., J. A. Battjes, and A. R. van Dongeren, 2003. Long waves induced by short-wave groups over a sloping bottom, *Journal of Geophysical. Research: Oceans,* 108(C8), 3252, doi:10.1029/2002JC001515

Marche, F., Bonneton, P., Fabrie, P. and Seguin, N., 2007. Evaluation of well-balanced bore-capturing schemes for 2D wetting and drying processes. *International Journal for Numerical Methods in Fluids* 53 (5), 867-894.

Michallet, H., *et al.*, 2014. GLOBEX: Wave dynamics on a shallow sloping beach, in *Proceedings of the HYDRALAB IV Joint User Meeting*,Lisbon.

van Noorloos, J. C., 2003. Energy transfer between short wave groups and bound long waves on a plane slope. *Master's thesis, Delft University of Technology, Delft, The Netherlands.*

Ruessink, B. G., M. G. Kleinhans, and P. G. L. Van den Beukel, 1998. Observations of swash under highly dissipative conditions, *Journal of Geophysical. Research*, 103(C2), 3111–3118.

Ruessink, G., H. Michallet, P. Bonneton, D. Mouaze, J. L. Lara, P. A. Silva, and P. Wellens, 2013. GLOBEX: Wave dynamics on a gently sloping laboratory beach, *in Proceedings of the Conference on Coastal Dynamics*, pp. 1351–1362, Arcachon, France.

Sénéchal, N., Bonneton, P. and Dupuis, H., 2001a. Field observations of irregular wave transformation in the surf zone, in *Proceedings of Coastal Dynamics*, pp. 64-74.

Sénéchal, N., Dupuis, H., Bonneton, P., Howa, H., and Pedreros, R., 2001b. Observation of irregular wave transformation in the surf zone over a gently sloping sandy beach on the French Atlantic coastline. *Oceanologica Acta*, *24*(6), 545-556.

Tissier, M., Bonneton, P., Michallet, H., and Ruessink, B. G., 2015. Infragravity-wave modulation of short-wave celerity in the surf zone. *Journal of Geophysical Research: Oceans*, *120*(10), 6799-6814.